

Comparison of paradigmatic gravity wave models for ocean and atmosphere

Uwe Harlander

Department of Aerodynamics and Fluid Mechanics
Brandenburg University of Technology Cottbus-Senftenberg

EGU2020-7222

<https://doi.org/10.5194/egusphere-egu2020-7222>

EGU General Assembly 2020

© Author(s) 2020. This work is distributed under the Creative Commons Attribution 4.0 License.



Comparison of paradigmatic gravity wave models for ocean and atmosphere

Uwe Harlander

Brandenburg University of Technology (BTU) Cottbus, Aerodynamics and Fluid Mechanics, Cottbus, Germany (haruwe@b-tu.de)

It appears that oceanographers and meteorologists have different pictures in their minds when they speak about internal waves. The reason might be that in both communities different paradigmatic gravity wave models based on different simplifying assumptions are in use. For the oceanographer, internal wave beams are rather common, a feature virtually unknown to the atmospheric scientist. In contrast, wave packets traveling upwards in the atmosphere is the standard picture for the meteorologist. The mathematical origin of such a different view is that for time harmonic waves, the underlying boundary value problem for internal waves in the ocean is hyperbolic but elliptic for atmospheric flows.

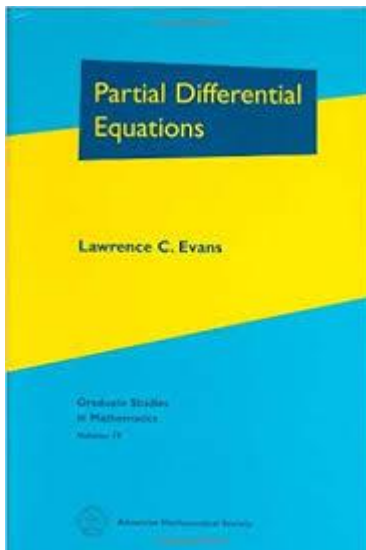
In the present paper we discuss the consequences that result from these two different types of boundary value problems. Wave focusing is a rather generic process for hyperbolic problems and we argue that the latter should also be of interest to meteorologists in view of new findings that indeed a significant part of the internal waves in the atmosphere travel downward. We further apply some of our findings to new laboratory data on inertial modes arguing that an additional shear flow leads to an elliptic boundary value problem and beam-like wave fields, typical for the inertial waves without a shear flow, become mode-like.

Type of a partial differential equation

For second order linear partial differential equations (PDEs)

$$Au_{xx} + Bu_{xy} + Cu_{yy} + Du_x + Eu_y + Fu = G, \quad (1)$$

with constants A to G , dependent variable $u = u(x, y)$, and independent variables x and y , the sign of $B^2 - 4AC$ determines whether the equation is elliptic $B^2 - 4AC < 0$, hyperbolic $B^2 - 4AC > 0$, or parabolic $B^2 - 4AC = 0$. For each type there is a pivotal example: the wave equation is hyperbolic, the Laplace equation is elliptic, and the heat equation is parabolic.



For more information the reader might consult a textbook on partial differential equation. A good source is the book shown to the left.

Stratified flow \mathbf{U} in the x - z plane:

The Boussinesq equations linearized around the basic state with $[u, w, p, \rho] = [U(z), 0, p_0(z), \rho_0(z)]$ read

$$\begin{aligned}\rho_0\left(\frac{\partial}{\partial t} + U\frac{\partial}{\partial x}\right)u + \rho_0 w \frac{dU}{dz} &= -\frac{\partial p}{\partial x} \\ \rho_0\left(\frac{\partial}{\partial t} + U\frac{\partial}{\partial x}\right)w + \rho_g &= -\frac{\partial p}{\partial z} \\ \frac{\partial u}{\partial x} + \frac{\partial w}{\partial z} &= 0 \\ \left(\frac{\partial}{\partial t} + U\frac{\partial}{\partial x}\right)\rho + w \frac{\partial \rho_0}{\partial z} &= 0.\end{aligned}$$

Using the definition $\tilde{D} = \frac{\partial}{\partial t} + U\frac{\partial}{\partial x}$ we yield

$$\tilde{D}^2 \nabla^2 \psi + N^2 \psi_{xx} = \tilde{D} \psi_x U_{zz}.$$

Here ψ is the streamfunction in the x - z plane.

Atmosphere

Typically, for the atmosphere we assume a stationary mean flow and the equation can be reduced to

$$\nabla^2 \psi + \lambda^2 \psi = 0,$$

with a constant

$$\lambda^2 = \frac{N^2}{U^2} - \frac{U_{zz}}{U}.$$

Obviously, this equation is elliptic.

Ocean

Typically, for the ocean we assume a zero mean flow but tidal oscillations with frequency ω and then the equation can be reduced to

$$\frac{\partial^2}{\partial z^2} \psi - \lambda^2 \frac{\partial^2}{\partial x^2} \psi = 0,$$

with

$$\lambda^2 = \frac{N^2 - \omega^2}{\omega^2}.$$

Obviously, this equation is hyperbolic for $\lambda^2 > 0$.

Solution for the atmospheric model

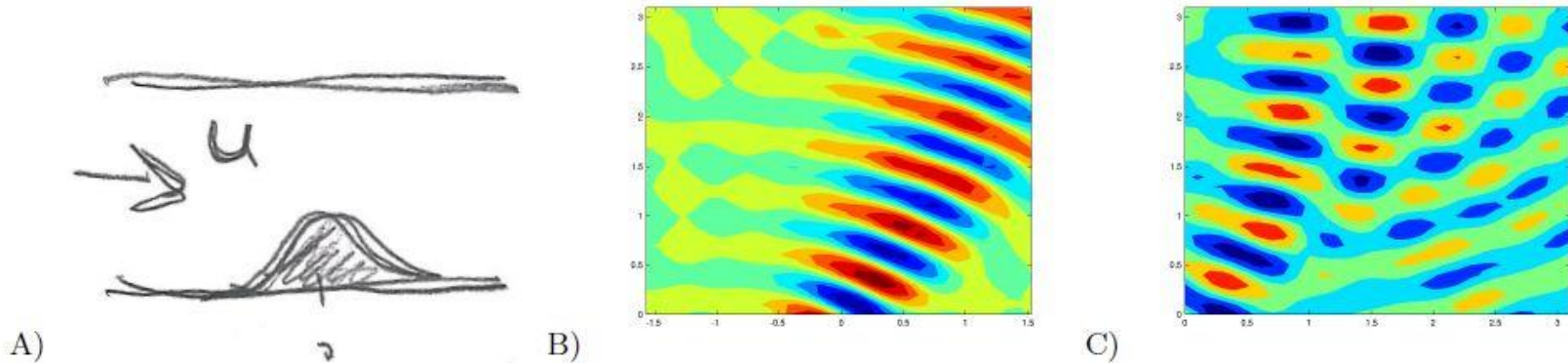


FIG. 1: A) Sketch of a horizontal flow towards a gaussian-shape topography. Periodic boundary conditions in the lateral direction are used. The top surface is either open or consists of a rigid wall. B) Stationary internal gravity wave field for an open upper surface in term of the vertical velocity. The topography is located at $x = 0$. The model parameters are $b = 10, N = 11, U = 1, N = 11, \lambda = N/U = 11$ implying real wave numbers. C) Stationary internal gravity wave field for a rigid upper surface at $z = \pi$ in term of the vertical velocity. Model parameters unchanged.

$$h(x) = \exp(-bx^2) \approx \sum_{k=1}^N a_k \cos(kx), \quad a_k = \frac{1}{2} \sqrt{\frac{\pi}{b}} \exp\left(\frac{-k^2}{4b}\right).$$

$$\psi = U \sum_{k=1}^N a_k \cos(kx + \sqrt{\lambda^2 - k^2}z),$$

Solution for the oceanic model

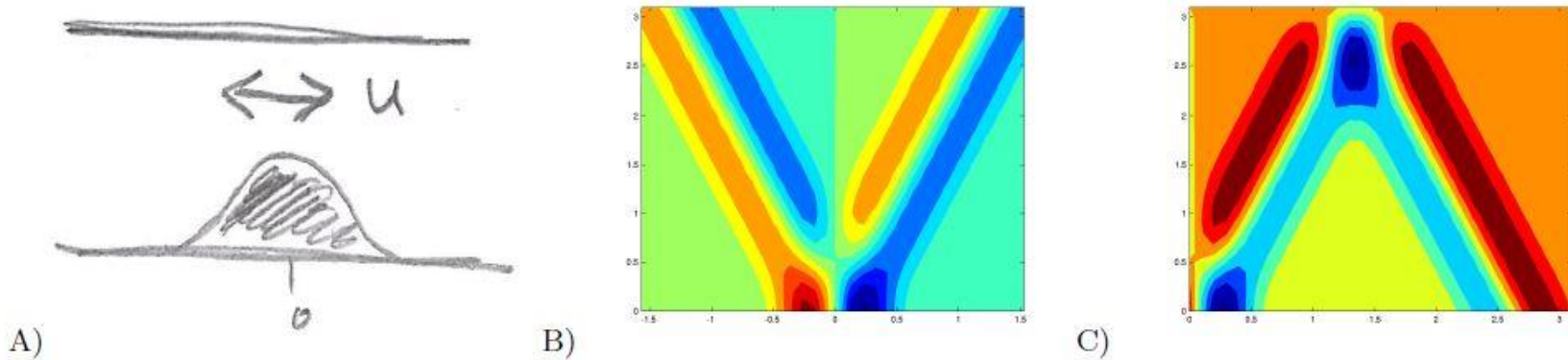


FIG. 3: A) Sketch of an oscillating flow over a gaussian-shape topography. Periodic boundary conditions in the lateral direction are used. The top surface is either open or consists of a rigid wall. B) Internal gravity wave beams for an open upper surface in term of the vertical velocity. The topography is located at $x = 0$. The model parameters are $b = 10$, $k_{max} = 100$, $N = 1$, $\omega = \sqrt{0.85}$ implying real wave numbers. C) Internal gravity wave beam for a rigid upper surface at $z = \pi$ in term of the vertical velocity. Model parameters unchanged.

$$\psi = \psi_0 \sum_{k=1}^N a_k \cos(k(x \pm \lambda z)).$$

In contrast to the elliptic atmospheric model, the oceanic model is NOT invariant with respect to a rotation of the coordinate system

Oceanic model for a frame rotated with the angle θ :

$$\frac{\partial^2}{\partial t^2} \nabla^2 \psi + N^2 \left(\cos^2 \theta \frac{\partial^2}{\partial x^2} + \sin^2 \theta \frac{\partial^2}{\partial z^2} - 2 \cos \theta \sin \theta \frac{\partial^2}{\partial x \partial z} \right) \psi = 0.$$

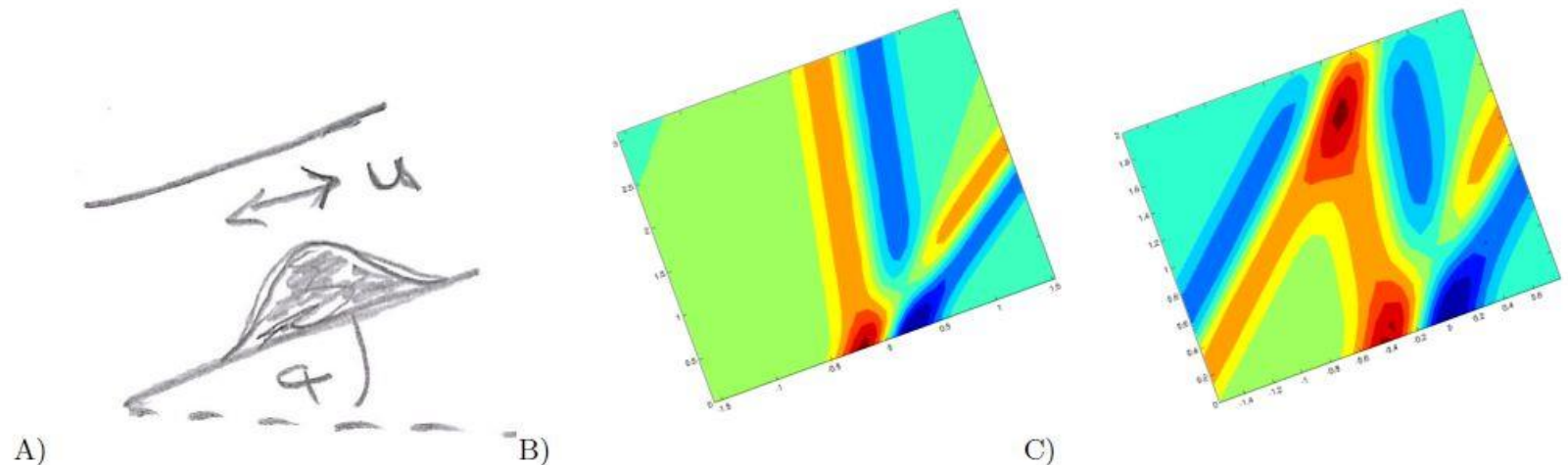


FIG. 4: Sketch of an upward horizontal flow towards a gaussian-shape topography. Here the channel has been rotated about the angle $\alpha = 20^\circ$.

Wave focusing is a consequence of this non-invariance:

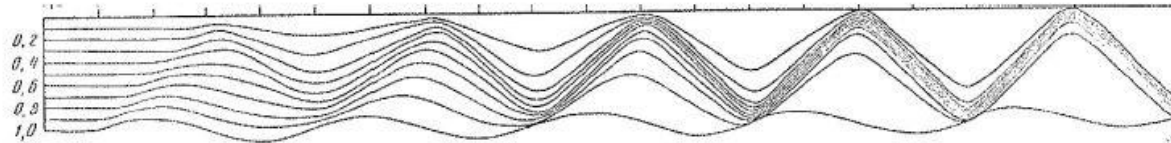
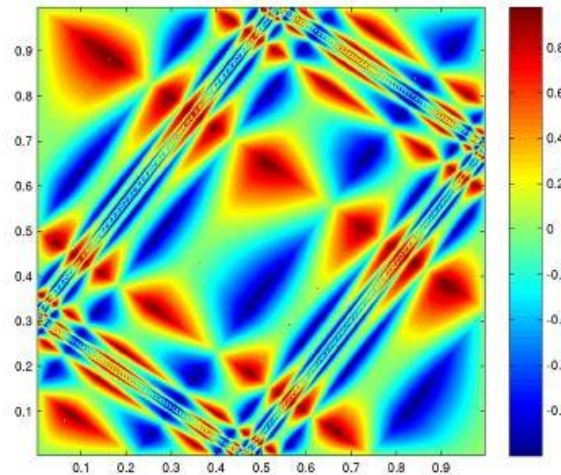


FIG. 5: Contours of the stream function for a sinusoidal bottom topography. Figure from V.A. Melnikov 1982, Effect of bottom relief on internal waves, Izvestiya, Atmospheric and Oceanic Physics, Vol. 18, No. 7, 603-606.

Extreme case: focusing in a closed and tilted domain leads to the formation of a wave attractor, i.e. a singularity in the velocity field.



*U. Harlander, I.D. Borcia, A. Krebs.
Nonnormality increases variance of
gravity waves trapped in a tilted box.
Geophys. & Astrophys. Fluid Dyn.
DOI:10.1080/03091929.2018.1549660,
2018.*

FIG. 6: Wave attractor. Fundamental intervals, $[0, 0.2543]$ $[0.7813, 1]$. Box is tilted over 9° . Frequency has been chosen such that internal wave rays have an angle of 45° in the non-tilted frame implying angles of 52° and 38° in the tilted frame.

Summary

Typical solutions of the atmospheric case are stationary wavepackets for which the mountain shape determines their structure.

For the oceanic case wave beams are typical. This is due to the fact that here an infinite number of waves exist that all have the same frequency. Superposing such waves gives the beam structure. Such a superposition is not possible for the simple stationary atmospheric flow case.

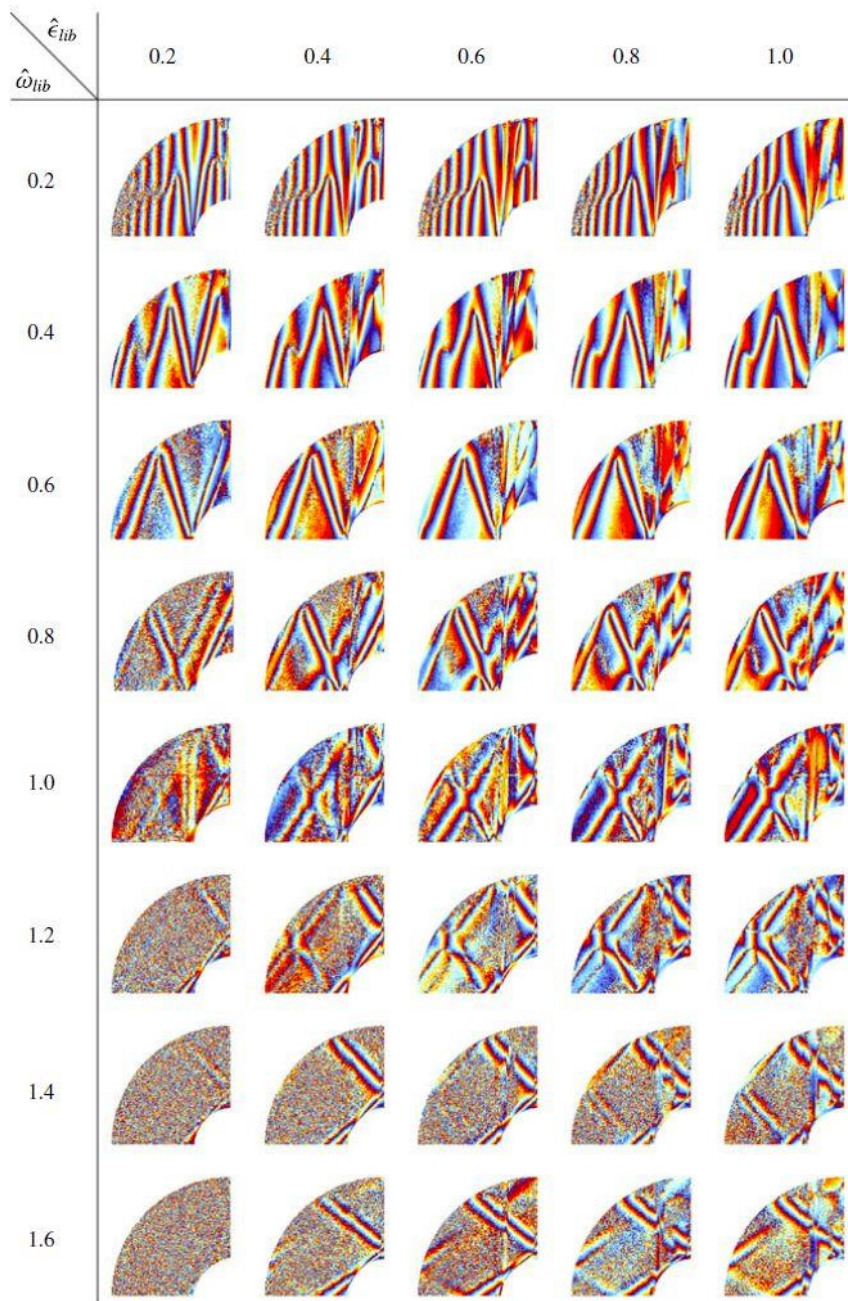
Whereas the Helmholtz equation (atmosphere) is invariant with respect to coordinate rotation, the Poincare equation (ocean) gives rise to new terms when the coordinates are rotated. In the rotated system, wave focusing is generic and has been observed in numerical and experimental data.

Outlook

In the discussion so far we pointed out that the type of the boundary value problem tells us a lot about the solution we can expect. In geophysical fluid dynamics this does not only hold for gravity waves but it has relevance in a broader context.

For rotating flows in closed containments we also find mode like solutions and solutions governed by wave beams. In the literature it is not sufficiently discussed why we can find such differences in cases that seem to be close.

On the next slides we will give examples.



Left we see a meridional section of a rotating spherical shell. Such a geometry has a large relevance for many geophysical problems. The results shown come from experimental data when the rotation of the spherical shell is modulated by frequency ω_{lib} and modulation amplitude ε_{lib} . Obviously, the flow in the shell is dominated by beams formed by a superposition of inertial waves. This situation is similar to the oceanic gravity wave case considered before.

More details can be found in

M. Hoff, U. Harlander, and C. Egbers. Experimental survey of linear and non-linear inertial waves and wave instabilities in a spherical shell. Journal of Fluid Mechanics, 789, 589-616, 2016.

FIGURE 4. (Colour online) Wave phases in the interval $[-\pi, \pi]$ of a harmonic analysis for different libration parameter settings. The Ekman number is $E \approx 4 \times 10^{-5}$.

The pattern below result from a similar experimental setup. This time a horizontal equatorial plane is displayed. In contrast to the experiment before, the inertial waves are not excited by a modulation but by rotating the inner sphere and the outer shell differentially. Hence the waves result from an instability of the driven shear flow. Obviously, the pattern we see correspond with smooth wave modes and not with beams. This situation is more similar to the atmospheric gravity wave case considered before.

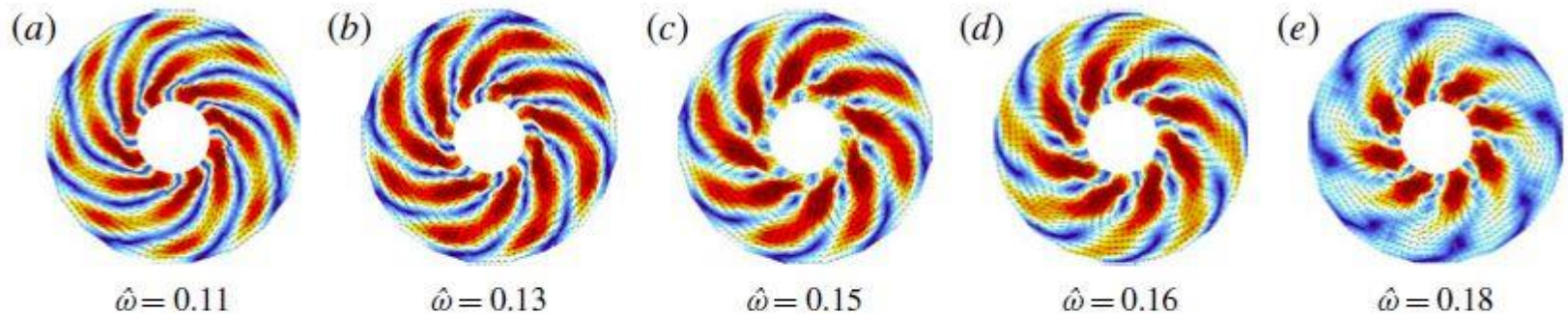
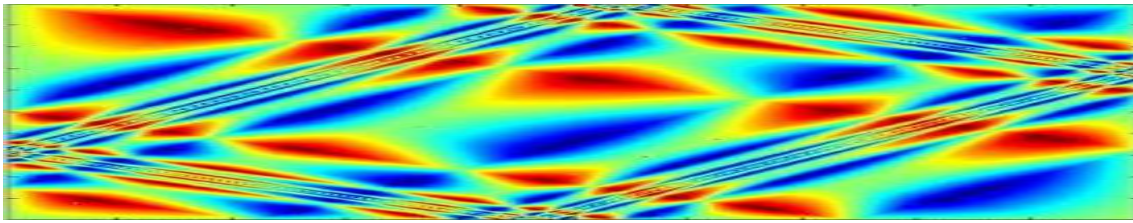


FIGURE 11. (Colour online) A series of five reconstructed patterns taken from the $m = 4$ branch in figure 7(b) for $\Omega_o = 60$ r.p.m., $E = 1.52 \times 10^{-5}$. From (a–e), $Ro = (0.18, 0.22, 0.25, 0.28, 0.31)$ and $|v|_{max} = (2, 2.5, 2.3, 1.7, 1.8)$ mm s⁻¹. The colours show the absolute value of velocity magnitude (blue – zero, red – max). The colour bar is scaled such that red is saturated in relation to the maximum velocity. The height of the horizontal plane is at $h = 4$ cm above the equator.



Conclusion

It is constructive to interpret solutions of boundary value problems with a view on the type of the underlying PDE. This seems to be a rather straightforward or even a trivial step. However, the consequences of such a change in type for the solutions in the case of confined fluids can be rather dramatic.

Typical but very different patterns of flows in seemingly close situations can be better understood taking into account the properties of hyperbolic boundary value problems that are not so well studied in literature.

U. Harlander and L.R.M. Maas. Two alternatives for solving hyperbolic boundary value problems in geophysical fluid dynamics. J. Fluid. Mech., 588, 331-351, 2007.

Theory is when you know
everything but nothing
works.

Practice is when everything
works but no one knows why.

In our lab, theory and
practice are combined:
nothing works and nobody
knows why.

Thanks for attention!

Thanks for support by



and



Brandenburg
University of Technology
Cottbus - Senftenberg